Metal-semiconductor transition in liquid-alkali-Te mixtures: *ab initio* molecular-dynamics simulations

2000 J. Phys.: Condens. Matter 12 A189

(http://iopscience.iop.org/0953-8984/12/8A/322)

J. Phys.: Condens. Matter **12** (2000) A189–A194. Printed in the UK PII: S0953-8984(00)08555-6

Metal–semiconductor transition in liquid-alkali–Te mixtures: *ab initio* molecular-dynamics simulations

K Hoshino†, F Shimojo† and Y Zempo‡

† Faculty of Integrated Arts and Sciences, Hiroshima University, Higashi-Hiroshima 739-8521, Japan

‡ Sumitomo Chemical, 6 Kitahara, Tsukuba 300-3294, Japan

Received 11 October 1999

Abstract. The structural and electronic properties of liquid Rb_xTe_{1-x} mixtures ($x = 0.0$, 0.2, and 0.5) are studied by *ab initio* molecular-dynamics simulations. It is shown that the transition from the metallic to the semiconducting state induced by adding Rb atoms is reproduced, and that this transition is related to the structural change in the Te chain. It is also shown from the calculated electronic density of states that almost complete charge transfer from Rb to Te occurs in the mixtures. The correlation between the spatial distribution of the transferred charge in the Te chains and the positions of Rb^+ ions is investigated.

1. Introduction

Though both crystalline Se and Te have trigonal chain structures and semiconducting character in the solid state, they have different features in the liquid state. Liquid Te is metallic, while liquid Se is semiconducting near the triple point. What is the difference between them?

As for liquid Se, the semiconductor–metal (SC–M) transition occurs when the temperature and the pressure are increased up to near the critical point [1, 2]. The structural change due to the SC–M transition was studied by x-ray diffraction [3, 4] and it was shown that the chain structure remains even in the metallic state, though the length of the chains becomes much shorter. Recently we [5,6] have clarified the microscopic mechanism of the SC–M transition on the basis of the structure and the electronic states obtained by our *ab initio* molecular-dynamics simulation.

On the other hand, the structure of liquid Te has been investigated by means of diffraction measurements [7–9] and it is known that there is no well-defined first coordination shell in the pair distribution functions, which suggests that there exists a high density of threefold-coordinated defects in the liquid phase. In an effort to understand the properties of liquid Te, some liquid-alkali–Te mixtures have also been studied experimentally [10–14] and it has been shown that a metal–semiconductor transition occurs when alkali elements are added to liquid Te. From these experiments, it is expected that the charge transfer from alkali elements to Te occurs in the liquid-alkali–Te mixtures. However, the spatial distribution of the transferred charge in the Te chains has not yet been investigated. Moreover, the microscopic atomic configuration of the Te chains and the alkali elements in the liquid-alkali–Te mixtures has never been studied theoretically.

In this paper, we present the results of our *ab initio* molecular-dynamics (MD) simulations of liquid-alkali–Te mixtures. The purposes of our study are:

0953-8984/00/SA0189+06$30.00

(i) to investigate the changes in the structure and the electronic states of liquid-alkali–Te mixtures with increasing alkali-element content, and
(ii) to clarify the microscopic mechanism of the metal–semiconductor transition on the basis of the atomic configuration, electronic density of states, and charge transfer obtained.

2. The method of calculation

Our method of calculation is based on the density-functional theory in which the generalized-gradient approximation [15] is used for the exchange–correlation energy. The wavefunctions are expanded in the plane-wave basis set and only the Γ point is used to sample the Brillouin zone of the supercell. The valence-electron configurations of the atoms Rb ($4p^6 5s^1$) and Te ($5s^2 5p^4$) are used in generating the ultrasoft pseudopotential [16]. The fractional occupation of each electronic state is taken into account, which is important near the Fermi level. The energy functional is minimized using an iterative scheme based on the preconditioned conjugate-gradient method [17–19], and the electronic charge density is obtained. Then the force acting on each ion is calculated by the Hellmann–Feynman theorem and the constant-temperature molecular-dynamics simulation [20, 21] is carried out using the force thus obtained to update the ionic configuration at the next time step.

The cubic supercell contains 80 atoms. Though we have carried out our simulation for liquid Rb–Te and K–Te mixtures, we only show here the results for liquid Rb–Te mixtures because of the lack of space. The simulations are carried out at three Rb concentrations: Rb_xTe_{1-x} with $x = 0.0$, 0.2, and 0.5. The temperatures and densities are (750 K, 0.0272 Å^{-3}), (710 K, 0.0196 Å^{-3}), and (710 K, 0.0177 Å^{-3}) for $x = 0.0$, 0.2, and 0.5, respectively. The time step is taken to be $\Delta t = 3.6 \times 10^{-15}$ s. The plane-wave cut-off energies for the wavefunctions and the charge density are 8.5 and 55 Ryd, respectively. The physical quantities are obtained by averaging over about 5 ps after the initial equilibration taking about 2 ps.

3. The atomic structure

In figure 1 we show the calculated structure factors, $S(k)$, for Rb_xTe_{1-x} with $x = 0.0$ and 0.2 in order to compare them with the experimental results [7,13,14]. No experimental measurements have been reported for $x = 0.5$. As is seen from the figure, the overall profile of the measured $S(k)$ of the pure liquid Te is reproduced fairly well by our simulation and the calculated $S(k)$ for liquid $Rb_{0.2}Te_{0.8}$ is in good agreement with the experiments. Though there is no structure on the low-k side of the main peak of $S(k)$, there exists a prepeak at around $k = 1.1$ Å^{-1} for the partial structure factor $S_{TeTe}(k)$, which is a so-called first sharp diffraction peak (FSDP). This FSDP also appears at around $k = 1.1$ Å^{-1} for the concentration–concentration structure factor $S_{cc}(k)$, which suggests some charge ordering in the liquid mixtures.

To examine how the structure changes with increasing Rb concentration in the liquid Rb–Te mixture, we show in figure 2 the calculated partial pair distribution functions $g_{ij}(r)$ for three Rb concentrations, $x = 0.0$, 0.2, and 0.5. It is seen from figure 2 that the overall profile of the measured $g(r)$ for liquid Te is reproduced fairly well by our simulation, in the sense that there is no well-defined first coordination shell in $g_{TeTe}(r)$ for the liquid Te. When the Rb concentration is increased, the first minimum of $g_{TeTe}(r)$ becomes deeper, and the first peaks of $g_{TeTe}(r)$ and $g_{RbTe}(r)$ become higher. As for $g_{RbRb}(r)$, it has broad distribution for both concentrations $x = 0.2$ and 0.5, though a plateau around 4.5 Å is recognized at $x = 0.5$.

To investigate the calculated chain structure of Te in the Rb–Te mixtures in more detail, we obtained the distribution function for the Te–Te coordination number (n), $P(n)$, as shown

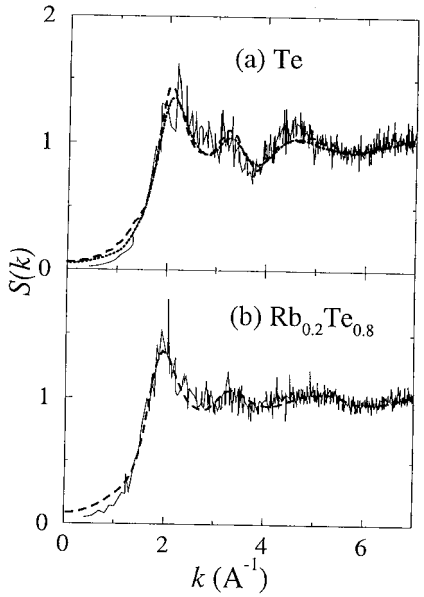

Figure 1. The structure factor $S(k)$ of liquid Rb_xTe_{1-x} for (a) $x = 0.0$ and (b) $x = 0.2$. The solid line shows the calculated result. The dashed and dotted lines show the results of neutron diffraction measurements by Kawakita *et al* [14] and Takeda *et al* [7], respectively.

in figure 3, which is calculated simply by counting the number of Te atoms inside a sphere of radius R (=0.31 nm) centred at each Te atom. $P(n)$ for pure liquid Te is largest at $n = 2$, and $P(3)$ is smaller than $P(2)$. For $x = 0.2$, the $P(n)$s for $n \geqslant 3$ decrease, and the $P(n)$s for $n \leqslant 2$ increase. This suggests that the interactions between Te chains are suppressed by the presence of alkali elements and that the twofold-coordinated chain structure is relatively stabilized. This is why a well-defined first coordination shell for the Te–Te pairs becomes evident when the Rb atoms are added. For $x = 0.5$, $P(n)$ has a peak at $n = 1$, which results from the large number of Te_2^{2-} dimers.

4. The electronic states

To investigate the change in the electronic states due to the structural change caused by adding the Rb atoms in the liquid Rb–Te mixtures, we calculate the electronic densities of states (DOS) for $x = 0.0$, 0.2, and 0.5, which are shown in figure 4. The origin of the energy is taken to be the Fermi level ($E_F = 0$). It is seen from figure 4(a) that the DOS is larger around E_F, i.e. pure liquid Te is metallic. As shown in figures 4(b) and 4(c), a dip at E_F in the DOS arises from the presence of Rb atoms, and the dip becomes deeper with increasing Rb concentration, which is consistent with the observed concentration dependence of the electrical conductivity [14]. Thus, we have succeeded in reproducing the metal–semiconductor transition in liquid Rb–Te mixtures with our *ab initio* MD simulations. It is found by decomposing the total DOS into the partial DOS that there are almost no states arising from the Rb 5s states, which means that almost complete charge transfer from Rb to Te occurs in the liquid Rb–Te mixtures.

In order to investigate the spatial distribution of transferred charge in the Te chains, we calculate the excess charge in the Te chains transferred from Rb atoms as

$$\Delta\rho(\boldsymbol{r}) = \rho(\boldsymbol{r}) - \rho_{\mathrm{Te}}(\boldsymbol{r}) - \rho_{\mathrm{Rb}}^{4\mathrm{p}}(\boldsymbol{r})$$

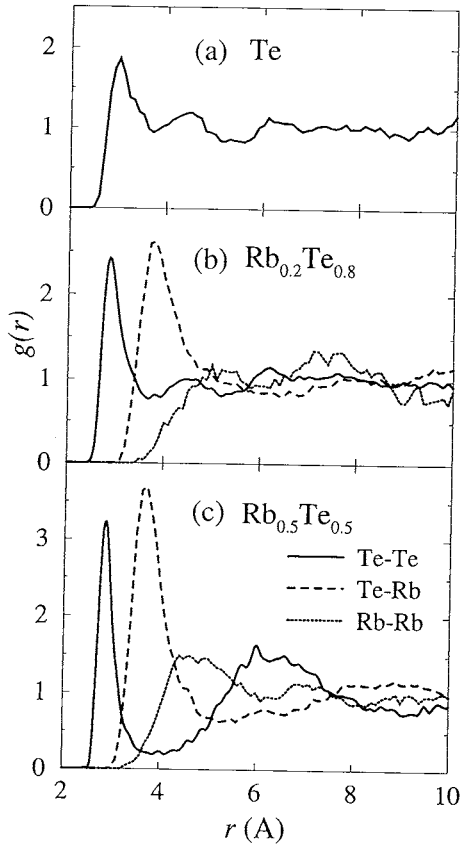

Figure 2. The partial pair distribution functions $g_{ij}(r)$ of liquid Rb_xTe_{1-x} for (a) $x = 0.0$, (b) $x = 0.2$, and (c) $x = 0.5$. The solid, dashed, and dotted lines show the calculated results for the Te–Te, Te–Rb, and Rb–Rb partial pair distribution functions, respectively.

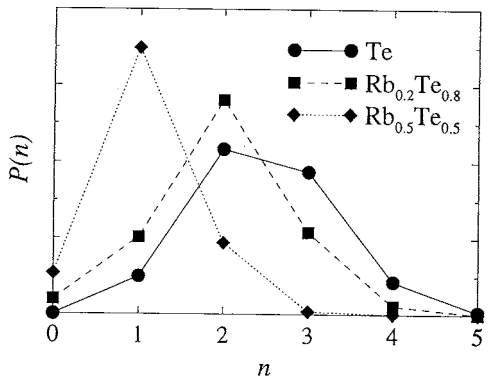

Figure 3. The Te–Te coordination number distribution function $P(n)$ of liquid Rb_xTe_{1-x} for $x = 0.0$, 0.2, and 0.5. The lines are drawn as guides to the eyes.

where $\rho(\boldsymbol{r})$ is the charge-density distribution for the liquid Rb–Te mixtures, $\rho_{\mathrm{Te}}(\boldsymbol{r})$ is the charge-density distribution obtained from a self-consistent electronic states calculation for a

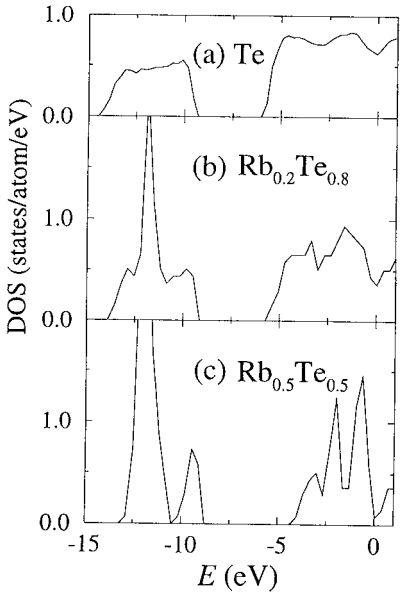

Figure 4. The electronic densities of states (DOS) of liquid Rb_xTe_{1-x} for (a) $x = 0.0$, (b) $x = 0.2$, and (c) $x = 0.5$. The origin of the energy is taken to be the Fermi level.

system containing only Te atoms which is obtained from the atomic configuration of the Rb–Te mixture by removing Rb atoms only, and $\rho_{Rb}^{4p}(\boldsymbol{r})$ is the charge-density distribution obtained by superposing the 4p electron-density distribution around Rb^+ ions. When we investigate the spatial distribution of $\Delta\rho(\boldsymbol{r})$ for $x = 0.5$, a 'dumb-bell-shaped' distribution around a pair of Te atoms is obtained, which was suggested by Fortner *et al* [11]. On the other hand, for $x = 0.2$, $\Delta\rho(\boldsymbol{r})$ distributes non-uniformly in the Te chains. To understand this feature in more detail, we define the total excess charge, ΔN_i, for the ith Te atom as

$$\Delta N_i = \int_{|\boldsymbol{r}-\boldsymbol{r}_i|\leqslant D} \mathrm{d}\boldsymbol{r}\ \Delta\rho(\boldsymbol{r}-\boldsymbol{r}_i)$$

where $\boldsymbol{r}_i$ is the position of the ith Te atom and D the radius of a sphere centred at each Te atom, and investigate the relation between ΔN_i and the Rb–Te distance R_i^{Rb-Te}, which is defined as the distance from the ith Te atom to its nearest Rb atom. It is found that ΔN_i increases with decreasing R_i^{Rb-Te}. Thus, in the case of $x = 0.2$, the distribution of the excess charge in the Te chains is very sensitive to the positions of neighbouring alkali atoms.

5. Summary

The structural and electronic properties of liquid Rb_xTe_{1-x} mixtures with $x = 0.0$, 0.2, and 0.5 have been studied by *ab initio* MD simulations. The calculated $S(k)$ and $g(r)$ are in reasonable agreement with the experimental results. The calculated electronic density of states (DOS) for liquid Te shows that the system has metallic properties. When the Rb atoms are added, a dip at E_F in the DOS appears, and the dip becomes deeper with increasing Rb concentration, which means that the metal–semiconductor transition in liquid Rb–Te mixtures has been successfully reproduced by our *ab initio* MD simulations. This metal–semiconductor transition is closely related to the structural change in the Te chain. For $x = 0.2$, the interactions between two Te

chains are suppressed by the presence of alkali elements, and as a result the twofold-coordinated chain becomes more stable. For $x = 0.5$, more than half of the Te atoms form Te_2^{2-} dimers. We conclude from the calculated DOS that almost complete charge transfer from Rb to Te occurs in the mixtures. At smaller Rb concentration, the excess charge transferred from Rb atoms distributes non-uniformly in the Te chains, according to the positions of neighbouring Rb atoms. At the equiatomic mixture, the excess charge has a 'dumb-bell-shaped' distribution around a pair of Te atoms as predicted by Fortner *et al* [11]. See Shimojo *et al* [22] for full details of this study.

Acknowledgments

We would like to thank Dr Y Kawakita, Professor M Yao, and Professor S Takeda for providing us with their experimental data. This work was supported by a Grant-in-Aid for Scientific Research from the Ministry of Education, Science, Sports, and Culture, Japan. We also wish to thank the Computer Centre of the Institute for Molecular Science for allowing us to use the NEC SX-3/34R supercomputer.

References

[1] Hoshino H, Schmutzler R W and Hensel F 1976 *Ber. Bunsenges. Phys. Chem.* **80** 27
[2] Hoshino H, Schmutzler R W, Warren W W Jr and Hensel F 1976 *Phil. Mag.* B **33** 255
[3] Tamura K and Hosokawa S 1992 *Ber. Bunsenges. Phys. Chem.* **96** 681
[4] Tamura K 1996 *J. Non-Cryst. Solids* **205–207** 239
[5] Shimojo F, Hoshino K, Watabe M and Zempo Y 1998 *J. Phys.: Condens. Matter* **10** 1199
[6] Hoshino K and Shimojo F 1998 *J. Phys.: Condens. Matter* **10** 11 429
[7] Takeda S, Tamaki S and Waseda Y 1984 *J. Phys. Soc. Japan* **53** 3830
[8] Munelle A, Bellissent R and Frank A M 1989 *Physica* B **156+157** 174
[9] Tsuzuki T, Yao M and Endo H 1995 *J. Phys. Soc. Japan* **64** 485
[10] Petric A, Pelton A D and Saboungi M-L 1988 *J. Chem. Phys.* **89** 5070
[11] Fortner J, Saboungi M-L and Enderby J E 1992 *Phys. Rev. Lett.* **69** 1415
[12] Fortner J and Saboungi M-L 1993 *Europhys. Lett.* **22** 359
[13] Kawakita Y, Yao M, Endo H and Dong J 1996 *J. Non-Cryst. Solids* **205–207** 447
[14] Kawakita Y, Yao M and Endo H 1997 *J. Phys. Soc. Japan* **66** 1339
[15] Perdew J P 1991 *Electronic Structure of Solids '91* ed P Ziesche and H Eschrig (Berlin: Akademie)
[16] Vanderbilt D 1990 *Phys. Rev.* B **41** 7892
[17] Arias T A, Payne M C and Joannopoulos J D 1992 *Phys. Rev.* B **45** 1538
[18] Kresse G and Hafner J 1994 *Phys. Rev.* B **49** 14 251
[19] Shimojo F, Zempo Y, Hoshino K and Watabe M 1995 *Phys. Rev.* B **52** 9320
[20] Nosé S 1984 *Mol. Phys.* **52** 255
[21] Hoover W G 1985 *Phys. Rev.* A **31** 1695.
[22] Shimojo F, Hoshino K and Zempo Y 1999 *Phys. Rev.* B **59** 3514